



**HAL**  
open science

# Effect of self-wetting fluids on the liquid/vapor phase change in a porous media of two-phase heat transfer devices

Riadh Boubaker, Souad Harmand, Safouene Ouenzerfi

## ► To cite this version:

Riadh Boubaker, Souad Harmand, Safouene Ouenzerfi. Effect of self-wetting fluids on the liquid/vapor phase change in a porous media of two-phase heat transfer devices. *International Journal of Heat and Mass Transfer*, 2019, 136, pp.655-663. 10.1016/j.ijheatmasstransfer.2019.03.016 . hal-03609128

**HAL Id: hal-03609128**

<https://uphf.hal.science/hal-03609128v1>

Submitted on 18 Nov 2024

**HAL** is a multi-disciplinary open access archive for the deposit and dissemination of scientific research documents, whether they are published or not. The documents may come from teaching and research institutions in France or abroad, or from public or private research centers.

L'archive ouverte pluridisciplinaire **HAL**, est destinée au dépôt et à la diffusion de documents scientifiques de niveau recherche, publiés ou non, émanant des établissements d'enseignement et de recherche français ou étrangers, des laboratoires publics ou privés.

# Effect of self-rewetting fluids on the liquid/vapor phase change in a porous media of two-phase heat transfer devices

Riadh Boubaker\*, Souad Harmand, Safouene Ouenzerfi

Laboratoire d'Automatique, de Mécanique et d'Informatique industrielles et Humaines (LAMIH), Université Polytechnique Hauts de France (UPHF), Le Mont Houy, F59313 Valenciennes CEDEX 9, France

## article info

**Keywords:**  
Phase change  
Porous media  
Self-rewetting fluids  
Visualization

## abstract

This paper presents an experimental study of the phase change phenomenon in a porous medium. The tested working fluids are pure water and butanol aqueous solutions with different concentrations. In contrast to ordinary fluids, the surface tension of self-rewetting fluids exhibits a positive gradient beyond a certain temperature value. The experimental results indicate that the use of self-rewetting fluids (water/butanol) as working fluid significantly improves the performance of the capillary evaporator by decreasing the casing temperature. To explain the heat transfer enhancement mechanism, the phase change phenomenon is visualized for the two working fluids. It is shown that as the applied power increases, the shape of the vapor pocket that developed within the porous wick also increases for pure water until it reaches a stable shape. With respect to self-rewetting fluids, the shape of the vapor pocket decreases with increasing applied power allowing more efficient mass and heat transfers. Wettability, capillary pressure and Marangoni forces are the factors related to surface tension and contact angle that seem to be responsible for this heat transfer improvement for self-rewetting fluids.

## 1. Introduction

The capillary pumped loop (CPL) and loop heat pipe (LHP) are passive two-phase heat transfer systems used for cooling electronic devices. These devices utilize the fluid circulation and vaporization phenomena that occur inside the porous wick to transport large heat loads without the need for a mechanical pump [1–5]. CPL and LHP systems are composed of an evaporator, a condenser, reservoir (compensation chamber), and vapor and liquid lines (see Fig. 1).

The evaporator, as shown in Fig. 2, is the major component of such devices, which is responsible for fluid circulation in the complete loop thanks to the capillary pressure generated inside the porous wick.

During steady-state or transient operations, a two-phase heat transfer system can encounter several heat transport limitations such as capillary limit, boiling limit and overheat limit. The capillary limit during the operation of the CPL and LHP is reached when pressure losses in the whole loop exceed the maximum capillary pressure generated inside the porous wick.

$$\Delta p_{tot} \geq \Delta p_{cap,max} \quad (1)$$

Assuming a spherical liquid/vapor interface, the maximum capillary pressure is defined by the Young-Laplace equation:

$$\Delta p_{cap,max} = \frac{2\sigma \cos \theta}{r_p} \quad (2)$$

where  $\sigma$  denotes the surface tension,  $r_p$  denotes the pore radius and  $\theta$  denotes the contact angle between the liquid and the wick. As for conventional heat pipes, the capillary limit is essentially related to the physical properties of the working fluid, particularly to the surface tension and to the wettability. For this reason, the choice of working fluid is important to overcome the abovementioned limitations and improve the thermal performance of two-phase heat transfer systems.

For ordinary fluids, surface tension always decreases with temperature, which has a detrimental effect on the thermal performance of two-phase heat transfer systems. However, for binary mixtures of fluids, called self-wetting fluids, the variation in surface tension as a function of temperature shows a positive slope from a certain temperature [7]. In the literature, many efforts have been devoted to study the influence of self-rewetting fluids on heat transfer systems performance. Savino et al. [8] studied numerically and experimentally the thermal performance of innovative heat pipes using binary mixtures. Their results indicated that heat pipes

\* Corresponding author.

E-mail addresses: [boubakker.riadh@yahoo.fr](mailto:boubakker.riadh@yahoo.fr) (R. Boubaker), [souad.harmand@univ-valenciennes.fr](mailto:souad.harmand@univ-valenciennes.fr) (S. Harmand).

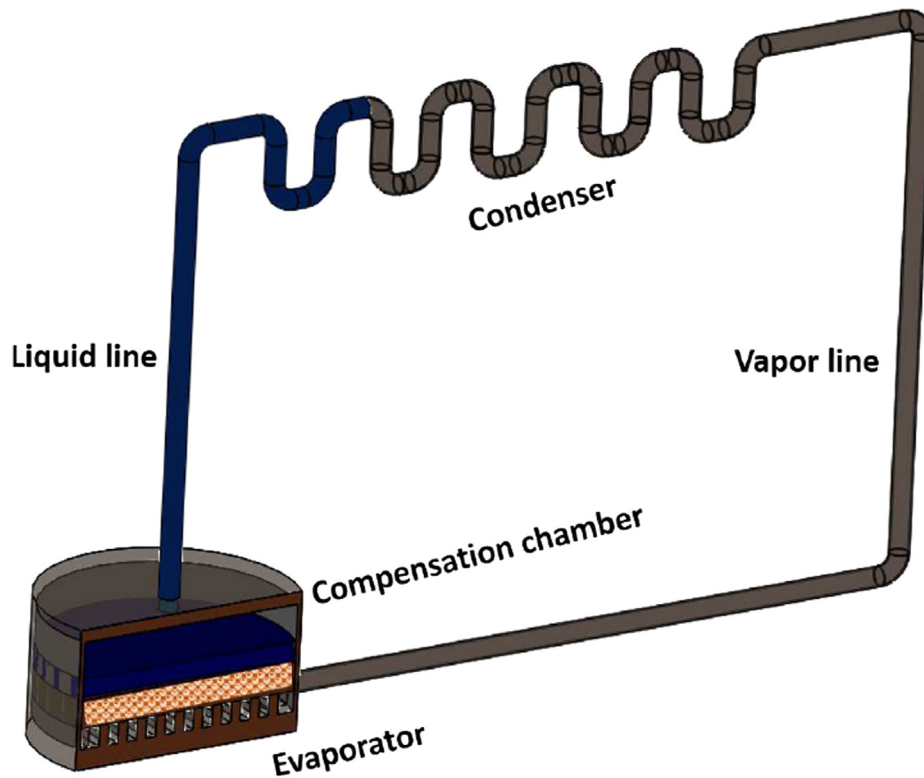


Fig. 1. LHP design [6].

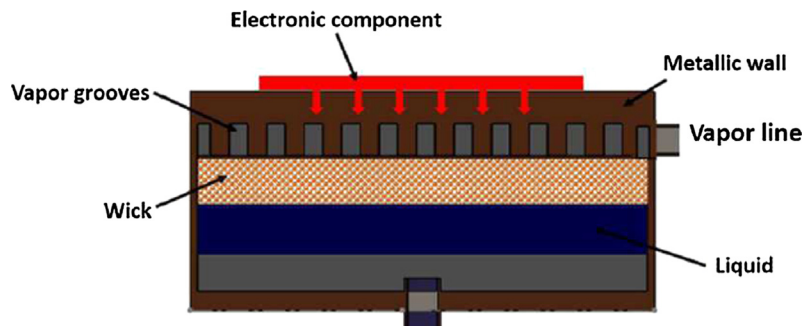


Fig. 2. Capillary evaporator [6].

filled with binary mixtures of fluids exhibit better thermal performance compared with heat pipes filled with pure water. Later, Savino et al. [9] experimentally studied the effect of Marangoni flow on the dry-out limit in heat pipe systems. Flow visualization has been performed for self-rewetting fluids, ordinary working fluids, and binary solutions having no minimum in surface tension. But, they reveal the difficulty of thermal measurement as well as the visualization of the phase change phenomenon. Fumoto et al. [10] studied the use of binary fluids in oscillating heat pipes. Experimental results showed that these working fluids greatly improve the maximum heat transport capacity and reduce thermal resistance. Leping Zhou et al. [11] studied the enhancement of pool boiling heat transfer in a porous structure formed by spherical glass beads. Experimental results showed that the bubble dynamics in water and aqueous n-butanol solution are different and varies with the applied power. The authors also showed that the superheat in the porous structure decreases with binary fluids owing to the unique interfacial properties of these fluids. Di Francescantonio et al. [12] analyzed the effect of heptanol aqueous

solution on the thermal performance of a heat pipe. They demonstrated that the use of an aqueous solution of heptanol as working fluid increases the dry-out limit of the heat pipe and considerably improves its thermal performance. The heat transfer enhancement is due to the Marangoni forces caused by the temperature gradient and concentration gradient, which provide an additional mechanism for the return of liquid from the condenser to the evaporator, other than capillary forces. Yanxin Hu et al. [13] studied the heat transfer enhancement of micro-oscillating heat pipes (MOHPs) by using binary fluids as a working fluid. Their experimental results showed that MOHPs filled with self-rewetting fluids (water/heptanol) exhibit low thermal resistance compared with water. Cecere et al. [14] conducted an experimental investigation of a flat plate pulsating heat pipe (FPPHP) under variable gravity conditions. Two working fluids were studied: an ordinary fluid (water) and a binary mixture (water/butanol). The authors demonstrated that, even at low heat flux, the FPPHP filled with pure water is not able to work under low gravity conditions owing to the evaporator dry-out. On the other hand, an FPPHP filled with self-rewetting fluids

still works during the microgravity phase and exhibits good thermal performance. Zhao et al. [15] studied the mechanism of heat and mass transfer of a large-scale oscillating heat pipe filled with self-rewetting fluid. They found that using self-rewetting fluid as a working fluid increases the heat transfer limit and reduces the thermal resistance of the heat pipe under large heating load, compared with water and ethanol. Naresh et al. [16] carried out experimental investigations on the thermal performance of internally-finned wickless heat pipes filled with different self-rewetting fluids. The authors concluded that all the self-rewetting fluids exhibit better performance compared with pure water. They also found that there is an optimum concentration that leads to the best performance of heat pipes for all working fluids. Peyghambarzadeh et al. [17] studied the heat transfer enhancement of circular heat pipes using self-rewetting fluid. Their results showed that heat pipes filled with aqueous solutions of butanol exhibit better thermal performance compared with those filled with water. Recently, Wu [18,19] carried out an experimental study on the influence of butanol aqueous solutions on the performance of LHP. The experimental results demonstrated that self-rewetting fluids reduce the operating temperature and total thermal resistance of LHPs, and improve heat transport capacity.

This paper presents an experimental study focusing on the impact of self-rewetting fluids (water/butanol) on heat and mass transfers in the porous wick of a two-phase capillary pumping loop. The novelty of this work lies in the analysis of the physical phenomena responsible for the improvement of heat and mass transfers inside the porous wick with self-rewetting fluids. The phase change phenomenon was visualized for aqueous solutions of butanol and pure water. If other works analyzed the effect of self-rewetting fluids on the global performance of two-phase heat transfer devices [20], in our work we studied separately the effect of such working fluids on the evaporator performance.

## 2. Experimental setup

### 2.1. Experimental procedure

The sketch of the experimental setup is shown in Figs. 3 and 4. It consists of a porous wick of copper foam and a grooved brass block to represent the flat evaporator section of a capillary two-phase loop. The experimental configuration also includes a transparent sapphire window. An infrared camera (FLIR SC7000 series (System overview: SC7200 – 7500/SC7300),  $320 \times 256$  pixels,  $30 \mu\text{m}$  detector pitch, range  $1.5\text{--}5.1 \mu\text{m}$ ) is installed in front of the sapphire/

porous interface that enables the visualization of the phase change on the surface (see Appendix A). To obtain a readable infrared image we have to respect  $50 \text{ mm}$  focus length following the macro  $50 \text{ mm}$  used Lens. Sapphire range transmission varies from  $0.17 \mu\text{m}$  to  $5.5 \mu\text{m}$  which is in a coherence to be transparent with the used IR camera. The upper surface of the porous structure is heated using a grooved brass block with cartridge heaters. Furthermore, the evaporator is heated from above and the vapor escapes upwardly (see Fig. 3). The heat losses due to the ambient environment are negligible since the heating block is thermally insulated with multilayered insulation materials (Bakelite, glass wool and polystyrene). The evaporator is connected to a constant-level reservoir to supply subcooled fluid to the wick under the same conditions. The hydrostatic pressure drop is controlled by the elevation  $\Delta h$ , the distance between the upper surface of the porous structure, and the water level in the reservoir. The liquid inside the reservoir is at ambient temperature, and thus a heating film is used to heat the liquid before it enters the porous wick. Two K-type thermocouples were used to measure the casing temperature  $T_c$  and the temperature of the fluid at the wick inlet  $T_{w,in}$ . The fluids considered in the present study are water and aqueous solutions of butanol with different concentrations.

### 2.2. Surface tension measurement

The surface tension of aqueous solutions of butanol and water was measured in the temperature range  $20\text{--}105 \text{ }^\circ\text{C}$  with the Kruss drop shape analyzer DSA30S using the pendant drop method (see Appendix B). This method is based on the Young-Laplace equation which relates the surface tension to the droplet shadow shape.

### 2.3. Contact angle measurement

The contact angles were measured for water and aqueous butanol solution at ambient temperature and for a substrate temperature of  $60 \text{ }^\circ\text{C}$  with the Kruss drop shape analyzer DSA30s, using the sessile drop method. Two substrates were tested: smooth copper substrate and porous copper substrate.

### 2.4. Error analysis

The temperatures of the liquid at the wick inlet and the casing were measured using K-type thermocouples. Measurement uncertainties are  $\pm 0.5 \text{ }^\circ\text{C}$ . With respect to the applied power, the relative uncertainty is estimated as  $1.1\%$ , which was determined using the following equation [21]:

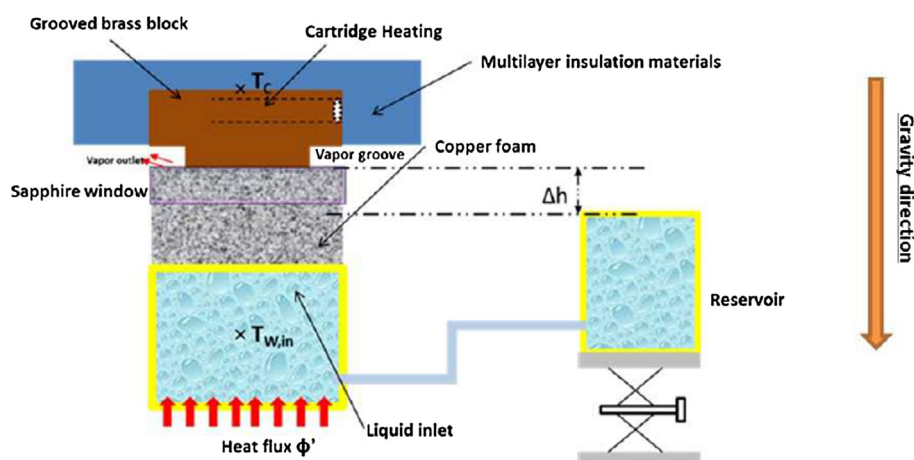


Fig. 3. Experimental setup [6].

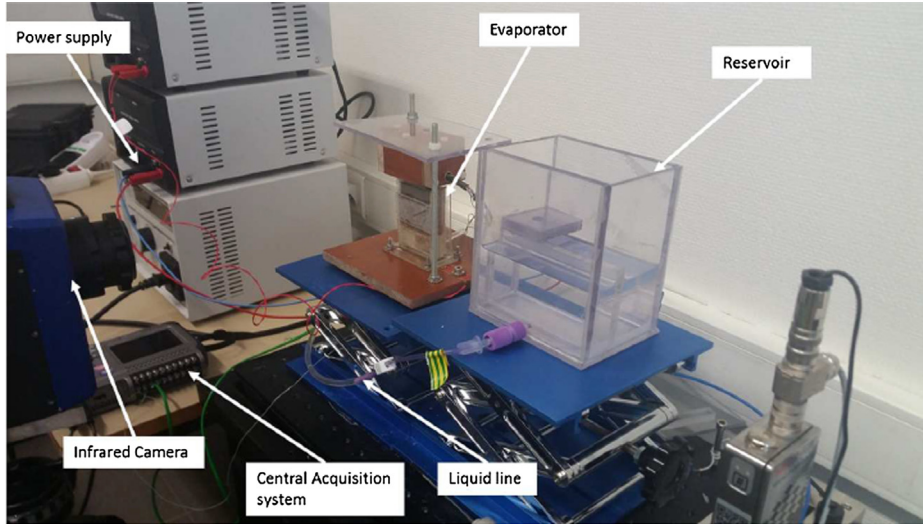


Fig. 4. Experimental setup in real site [6].

$$\frac{\delta\phi}{\phi} = \sqrt{\left(\frac{\delta V}{V}\right)^2 + \left(\frac{\delta I}{I}\right)^2}$$

where  $\phi$  denotes the applied heat load, V is the voltage and I is the current.

For contact angle measurements, the uncertainty is estimated as  $\pm 3$  deg.

#### 2.4.1. Thermal resistance

In order to describe the thermal performance of the evaporator, we define the evaporator thermal resistance as follows:

$$R_E = \frac{T_C - T_{W,in}}{\phi} \quad (3)$$

where  $\phi$  denotes the heat flux applied to the evaporator,  $T_C$  denotes the casing temperature and  $T_{W,in}$  denotes the liquid temperature at the wick inlet.

### 3. Results and discussion

#### 3.1. Porous media properties

The real sample of the copper wick structure is shown in Fig. 5 (the photo is taken by ESC microscope CCD camera). The dimensions of the porous wick are  $50 \times 50 \times 15 \text{ mm}^3$ . The properties of the wick are listed in Table 1. The effective thermal conductivity and permeability are respectively by thermal parallel model and Kozeny-Carman correlation.

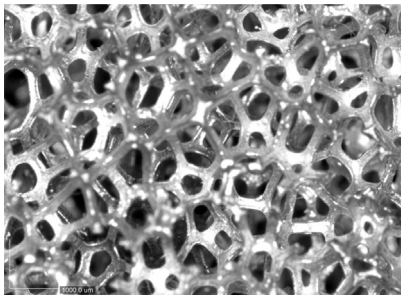


Fig. 5. Wick image.

Table 1

Porous media properties.

Mean pore diameter (mm)	0.635
Porosity (%)	96
Permeability ( $\text{m}^2$ )	$1.238 \cdot 10^{-6}$
Effective thermal conductivity (W/mK)	16.24

#### 3.2. Surface tension

Fig. 6 shows the evolution of the measured surface tension for water and self-wetting fluids (water/butanol) at different concentrations of butanol. The surface tension of water always decreases with temperature. However, for aqueous solutions of butanol, the surface tension has a positive slope when the temperature exceeds  $52 \text{ }^\circ\text{C}$ . It can also be seen that the surface tension varies with concentration. In particular, the surface tension decreases when we increase the butanol concentration.

#### 3.3. Heat transfer characteristics

Fig. 7 shows the variation in the casing temperature as a function of the applied power for pure water and aqueous solutions of butanol with different concentrations as working fluids. This figure shows that as the heat load increases, the temperature of the evaporator also increases. For butanol aqueous solutions, the casing temperature is always lower than that of water. During the operation of an evaporator filled with a self-wetting fluid, the casing temperatures are approximately  $120 \text{ }^\circ\text{C}$  and  $143 \text{ }^\circ\text{C}$  for the 3% and 5% concentrations respectively; for the water, the temperature is approximately  $154 \text{ }^\circ\text{C}$  for a heat load of  $82 \text{ W}$ . The self-wetting fluid with a concentration of 3% exhibits the best performance. The overheat in the evaporator casing is higher for water because the vapor pocket that developed inside the porous wick is larger.

Fig. 8 describes the temperature evolution of the casing temperature for different working fluids at steady state. It can be seen that the difference in temperature between butanol aqueous solutions and water increases with the heat load. This can be explained by the fact that the surface tension for water always decreases when the temperature increases.

The variation in the thermal resistance as a function of the applied power for butanol aqueous solutions and water is shown



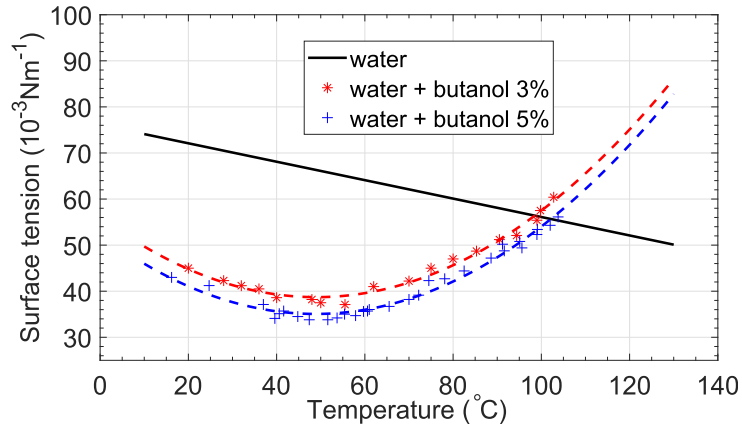


Fig. 6. Surface tension measurements for water and aqueous solutions of butanol.

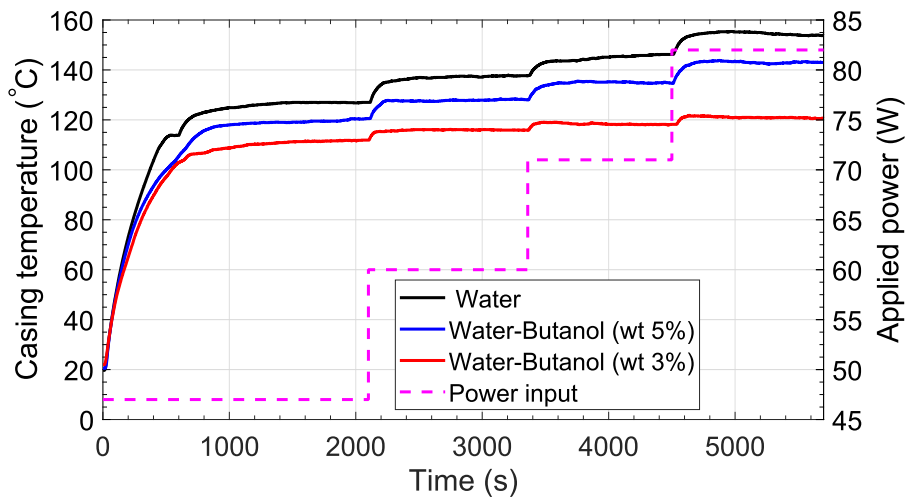


Fig. 7. Temporal evolution of the casing temperature for water and self-rewetting fluids.

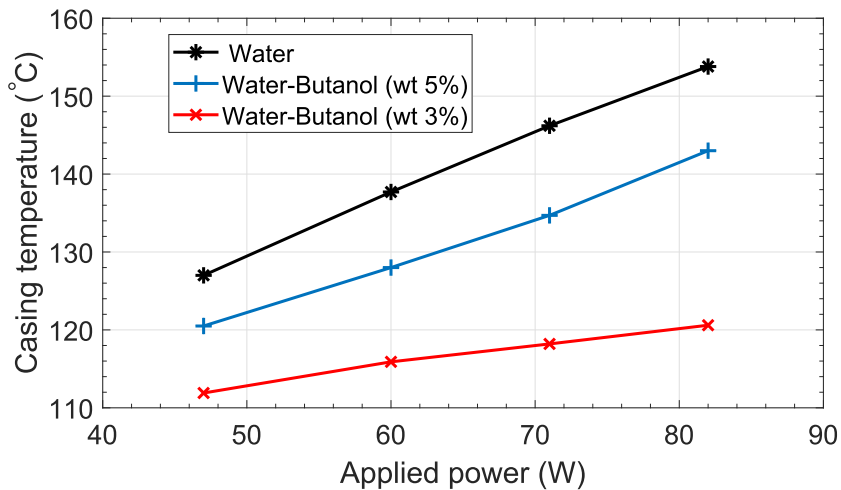


Fig. 8. Evolution of the casing temperature for water and self-rewetting fluids.

in Fig. 9. It can be seen that the use of self-rewetting fluids reduces the thermal resistance of the evaporator. Indeed, for an applied power of 82 W, the thermal resistance for the aqueous solution of butanol (wt 3%) is approximately 28% lower than that of pure water.

### 3.4. Vapor pocket dynamics

In order to understand the enhancement of the thermal performance of the evaporator with self-rewetting fluids, the liquid/vapor phase change was visualized. Infrared emissivities of liquid,

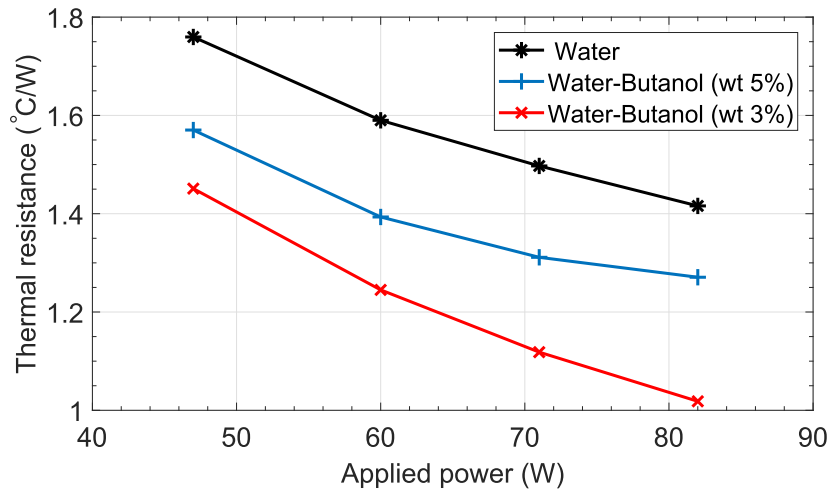


Fig. 9. Thermal resistance for water and self-rewetting fluids.

vapor/solid are different at a given temperature. By consequence, it induces different temperature ranges colors on the IR detector, which enables the location of the liquid/vapor interface by IR thermal imaging. Fig. 10 depicts the evolution of the vapor pocket as a function of the applied power for water and aqueous solution of butanol (wt 3%) as working fluids. It can be seen that the size of the vapor pocket increases with the applied power until it exhibits a nearly stable shape for water, regardless of the heat load applied

to the evaporator envelope. This result can be explained as follows. The increase in the heat load causes a higher vapor mass flow rate at the outlet of the evaporator. As a result, the mass flow rate of the liquid at the outlet of the reservoir also increases, resulting in a lower liquid temperature at the inlet of the wick. Both of these effects tend to stabilize the vapor pocket within the capillary structure. This result is in agreement with the numerical results of Bou-baker [22] and Ren [23]. The vapor pocket that developed within

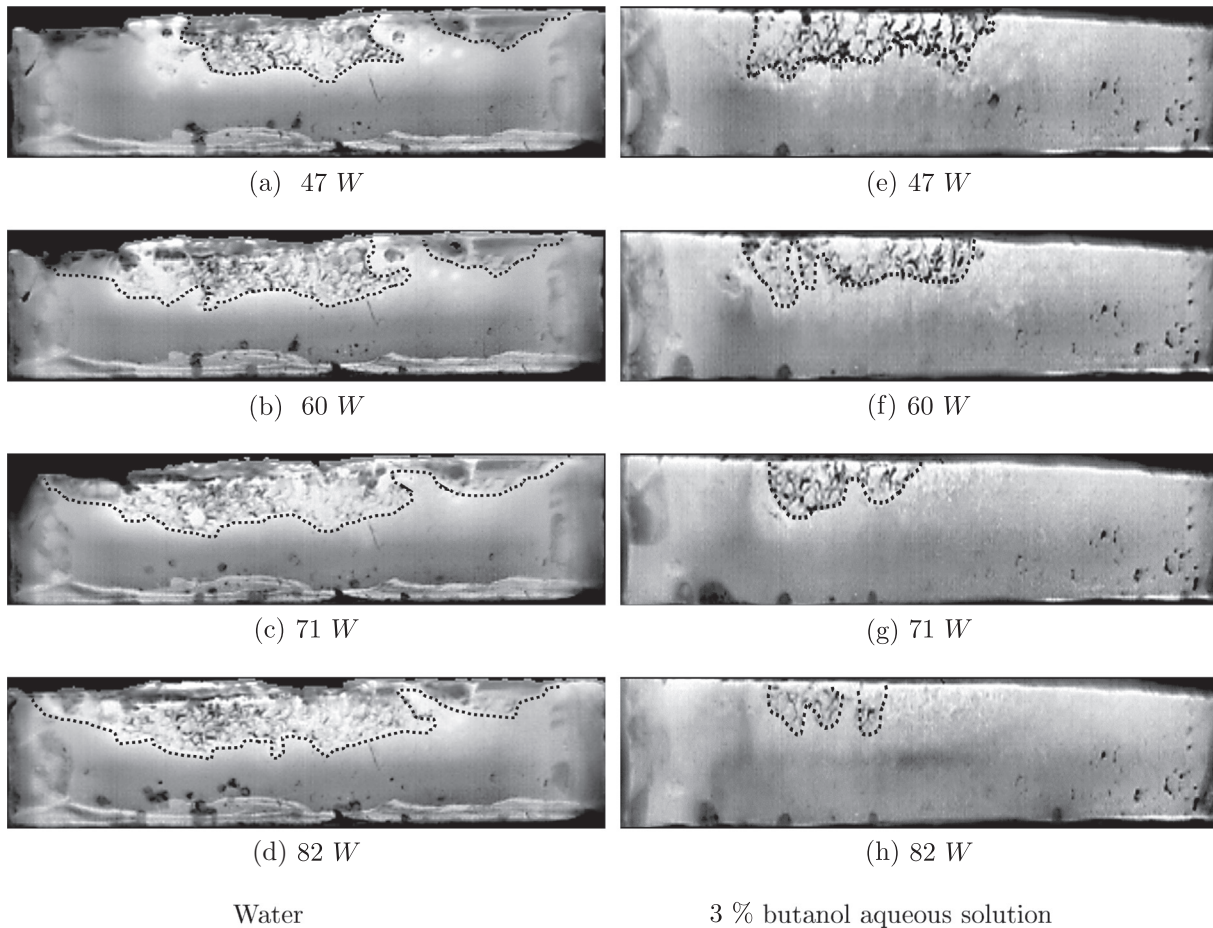


Fig. 10. Comparison of the vapor pocket for water and self-rewetting fluids water/butanol (wt 3%).

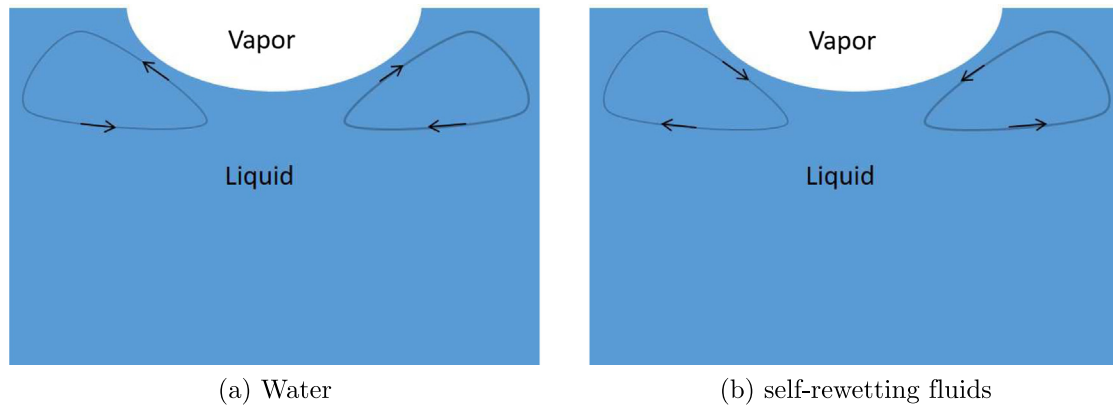


Fig. 11. Marangoni effect.

the porous wick causes high thermal resistance, which promotes overheating of the evaporator casing and affects the thermal performance of the evaporator. Unlike water, the vapor zone, comprising the depth and diameter, decreases within the wick with increasing the applied power for 3% butanol aqueous solution. Thus, the thermal resistance of the vapor pocket inside the capillary structure decreases, which explains the decrease in the casing temperature of the evaporator and the increase in thermal performance of the evaporator when it is filled with a self-wetting fluid.

### 3.5. Phenomena responsible of improving heat transfer with self-wetting fluids

The improvement in the thermal performance of the evaporator for the water-butanol binary mixture comes mainly from the physical phenomena associated with the surface tension and contact angle: capillarity, Marangoni forces, and wettability.

#### 3.5.1. Capillary forces

Capillary forces play a very important role in the operation of two-phase pumped loops; they are responsible for the circulation of fluid in the whole loop. As mentioned above, the capillary pressure is proportional to the surface tension. When the surface tension is high, the capillary pressure is large and the vapor pocket is small.

For 3% butanol aqueous solutions, the surface tension of the self-wetting fluid exceeds that of water when the temperature exceeds 99 °C. From this temperature, capillary pumping is more important for butanol aqueous solutions (wt 3%). This explains the decrease in the size of the vapor pocket as a function of the applied heat load for the self-wetting fluid (Fig. 10). When the vapor pocket is small, the evaporator casing becomes much less isolated from the subcooled liquid feed, which enhances the heat transfer inside the porous wick and decreases the casing temperature.

#### 3.5.2. Marangoni forces

The Marangoni effect takes place when there is a surface tension gradient which can be the result of the existence of a temperature and/or concentration gradient. The Marangoni convection is

called thermal Marangoni in the case of a temperature gradient, and solutal Marangoni in the case of a concentration gradient. The thermal and solutal Marangoni convection are respectively characterized by the following dimensionless numbers:

$$M_a^T = -\frac{d\sigma}{dT} \frac{L_c}{\mu\alpha} \Delta T$$

$$M_a^S = \frac{d\sigma}{dC} \frac{L_c}{\mu D_B} \Delta C$$

where  $\sigma$  denotes the surface tension,  $L_c$  denotes the characteristic length,  $\alpha$  denotes the thermal diffusivity,  $\mu$  denotes the dynamic viscosity, and  $D_B$  denotes the diffusion coefficient.

Marangoni convection implies flows to the zone where the surface tension is high. Fig. 11 shows that in the case of pure water, such flow will be from hot region to cold region because the surface tension always decreases as a function of temperature (negative  $\frac{d\sigma}{dT}$ ). This flow will increase in the temperature of the fluid inside the porous wick and the casing temperature of the evaporator.

For self-wetting fluid, in contrast to the ordinary liquid, the surface tension has a positive gradient from 50 °C (see Fig. 6: positive  $\frac{d\sigma}{dT}$ ). In this case, the reverse Marangoni flow drives liquid from cold regions to hot regions. As shown in Fig. 11, the surface tension gradient along the liquid-vapor interface, caused by both the temperature and concentration gradients, induce a flow that feeds the liquid-vapor interface with cold liquid. Therefore, the size of the vapor pocket that developed inside the porous wick decreases and the casing temperature is significantly reduced.

#### 3.5.3. Wettability

In order to explain the improvement of the heat transfer in the porous medium with self-wetting fluids, an additional experiment was carried out to evaluate the effect of the working fluid, the nature of the substrate, and the substrate temperature on the contact angle. Table 2 shows a comparison of contact angle between water and the water-butanol binary mixture (wt 5%) at two different substrate temperatures for smooth and porous copper substrates. Experimental data indicate that the addition of a small amount of alcohols, particularly butanol, significantly

Table 2  
Contact angle (deg).

Fluids	$T_{sub} = 20\text{ }^\circ\text{C}$		$T_{sub} = 60\text{ }^\circ\text{C}$	
	Smooth copper	Porous copper	Smooth copper	Porous copper
Water	79.4	71.3	53.7	77.8
Water/Butanol wt 5%	36.5	20.5	23.9	Spontaneous spreading



decreases the contact angle and improves the wettability of the self-rewetting fluids with metals, regardless of the nature of the substrate: smooth or porous substrate. Wetting surfaces lead to high conduction of heat between the solid and working fluid, and enhances heat transfer inside the porous wick.

It was difficult to measure the contact angle of the water-butanol binary mixture for the porous copper substrate at 60 °C. Indeed, a drop of the self-rewetting fluid spreads easily and quickly on the porous substrate, which means that the contact angle for water-butanol (wt 5%) at 60 °C is zero.

#### 4. Conclusion

In this work, we experimentally investigated the impact of self-rewetting fluids (water/butanol) on heat and mass transfer in the porous media of two-phase heat transfer devices. In order to improve the understanding of heat transfer enhancement with self-rewetting fluids, the liquid/vapor phase change was visualized, and an additional experiment was carried out to measure the surface tension and contact angle for water and binary mixture water/butanol. The broad conclusions from this work are as follows:

1. The use of self-rewetting fluids decreases the casing temperature and thermal resistance of the capillary evaporator.
2. The temperature of the evaporator increases with increasing the concentration of butanol in aqueous solutions of butanol.
3. The size of the vapor pocket that developed inside the porous wick for pure water increases with increasing applied power until it reaches a stable shape.
4. For self-rewetting fluids, the vapor pocket size decreases with increasing applied heat load, which explains the significant enhancement of the evaporator thermal performance.

5. The addition of butanol considerably improves the wettability between self-rewetting fluids and the wick structure, and enhances the heat conduction between liquid and solid.
6. The origin of the different behaviors of water and self-rewetting fluids comes mainly from the phenomena of capillarity, Marangoni and wettability associated with surface tension and contact angle.
7. If adding butanol concentration will enhance the thermal performance of the fluid compared to the water one, qualifying the optimum value of this concentration is not evident. Indeed, increasing butanol concentration improves wettability but deteriorates the surface tension and thermo-physical properties. New experiment has to be set with several concentrations of n-butanol aqueous solutions to identify the optimal concentration leading to the best thermal performance.

#### Conflict of interest

The authors declared that there is no conflict of interest.

#### Acknowledgements

This work has been achieved within the framework of CE2I project (Convertisseur d'Énergie Intégré Intelligent). CE2I is co-financed by European Union with the financial support of European Regional Development Fund (ERDF), French State and the French Region of Hauts-de-France.

#### Appendix A. Technical FLIR specification

See Fig. A.12.



<b>System Overview</b>	<b>SC7210-7500 / SC7300</b>
Waveband	MW
Sensor type	InSb / MCT
Pixel Resolution	320x256
Pixel Pitch	30µm
Spectral ranges	1.5 - 5.1 µm for InSb (BB)
<b>Measurement</b>	
NETD	<20mK for InSb
Standard Camera Calibration Range	5°C to 300°C for InSb
Optional Camera Calibration Range	-20°C to 300°C
Digital Full Frame rate	InSb: 190 Hz - 380 Hz full frame up to 3 kHz - 39.8 kHz with windowing

Fig. A.12. Technical FLIR specification.

## Appendix B. KRUSS chamber for surface tension measurements

See Fig. B.13.

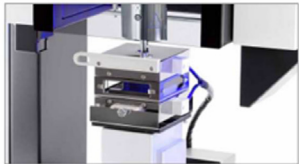
TC21 – TEMPERATURE CONTROLLED CHAMBER FOR HIGH TEMPERATURES	DS30 SPECIFICATIONS														
	<b>Pendant drop/rising drop</b>														
	<table border="1"> <tr> <td>Results</td> <td>interfacial and surface tension</td> </tr> <tr> <td>Range</td> <td>0.01 to 2000 mN/m</td> </tr> <tr> <td>Resolution</td> <td>0.01 mN/m</td> </tr> <tr> <td>Accuracy</td> <td>0.3 mN/m</td> </tr> <tr> <td>Model</td> <td>Young-Laplace</td> </tr> <tr> <td>Types</td> <td>Static, dynamic</td> </tr> </table>	Results	interfacial and surface tension	Range	0.01 to 2000 mN/m	Resolution	0.01 mN/m	Accuracy	0.3 mN/m	Model	Young-Laplace	Types	Static, dynamic		
Results	interfacial and surface tension														
Range	0.01 to 2000 mN/m														
Resolution	0.01 mN/m														
Accuracy	0.3 mN/m														
Model	Young-Laplace														
Types	Static, dynamic														
<p>The temperature controlled chamber TC21 enables liquid and solid surfaces to be analyzed at temperatures up to 400 °C.</p>	<b>Temperature control</b>														
	<table border="1"> <tr> <td>Equipment</td> <td>temperature-controlled sample stage, chambers, cuvette</td> </tr> <tr> <td>Types</td> <td>liquid, electrical, Peltier</td> </tr> <tr> <td>Range</td> <td>-30 to 400 °C</td> </tr> <tr> <td>Maximum sample size</td> <td>132 mm × 132 mm × 27 mm (W × D × H)</td> </tr> <tr> <td>Resolution</td> <td>0.1 K</td> </tr> <tr> <td>Flow-through thermostat</td> <td>With liquid</td> </tr> <tr> <td>Inert gas</td> <td>Yes</td> </tr> </table>	Equipment	temperature-controlled sample stage, chambers, cuvette	Types	liquid, electrical, Peltier	Range	-30 to 400 °C	Maximum sample size	132 mm × 132 mm × 27 mm (W × D × H)	Resolution	0.1 K	Flow-through thermostat	With liquid	Inert gas	Yes
Equipment	temperature-controlled sample stage, chambers, cuvette														
Types	liquid, electrical, Peltier														
Range	-30 to 400 °C														
Maximum sample size	132 mm × 132 mm × 27 mm (W × D × H)														
Resolution	0.1 K														
Flow-through thermostat	With liquid														
Inert gas	Yes														

Fig. B.13. KRUSS chamber for surface tension measurements.

### References

- [1] E. Pouzet, J.-L. Joly, V. Platel, J.-Y. Grandpeix, C. Butto, Dynamic response of a capillary pumped loop subjected to various heat load transients, *Int. J. Heat Mass Transf.* 47 (10) (2004) 2293–2316.
- [2] R. Boubaker, V. Platel, Dynamic model of capillary pumped loop with unsaturated porous wick for terrestrial application, *Energy* 111 (2016) 402–413.
- [3] R. Boubaker, V. Platel, S. Harmand, A numerical comparative study of the effect of working fluids and wick properties on the performance of capillary pumped loop with a flat evaporator, *Appl. Therm. Eng.* 100 (2016) 564–576.
- [4] Y. Maydanik, Loop heat pipes, *Appl. Therm. Eng.* 25 (5) (2005) 635–657.
- [5] G. Zhou, J. Li, Two-phase flow characteristics of a high performance loop heat pipe with flat evaporator under gravity, *Int. J. Heat Mass Transf.* 117 (2018) 1063–1074.
- [6] R. Boubaker, S. Harmand, V. Platel, Experimental study of the liquid/vapor phase change in a porous media of two-phase heat transfer devices, *Appl. Therm. Eng.* 143 (2018) 275–282.
- [7] Y. Hu, K. Huang, J. Huang, A review of boiling heat transfer and heat pipes behaviour with self-rewetting fluids, *Int. J. Heat Mass Transf.* 121 (2018) 107–118.
- [8] R. Savino, N. di Franciscantonio, R. Fortezza, Y. Abe, Heat pipes with binary mixtures and inverse Marangoni effects for microgravity applications, *Acta Astronaut.* 61 (1) (2007) 16–26.
- [9] R. Savino, D.D. Cristofaro, A. Cecere, Flow visualization and analysis of self-rewetting fluids in a model heat pipe, *Int. J. Heat Mass Transf.* 115 (2017) 581–591.
- [10] K. Fumotoa, M. Kawajib, T. Kawanamic, Study on a pulsating heat pipe with self-rewetting fluid, *J. Electron. Packag.* 132 (3) (2010) 031005.
- [11] L. Zhou, Z. Wang, X. Du, Y. Yang, Boiling characteristics of water and self-rewetting fluids in packed bed of spherical glass beads, *Exp. Therm. Fluid Sci.* 68 (2015) 537–544.
- [12] N. di Franciscantonio, R. Savino, Y. Abe, New alcohol solutions for heat pipes: Marangoni effect and heat transfer enhancement, *Int. J. Heat Mass Transf.* 51 (25) (2008) 6199–6207.
- [13] Y. Hu, T. Liu, X. Li, S. Wang, Heat transfer enhancement of micro oscillating heat pipes with self-rewetting fluid, *Int. J. Heat Mass Transf.* 70 (2014) 496–503.
- [14] A. Cecere, D.D. Cristofaro, R. Savino, V. Ayel, T. Sole-Agostinelli, M. Marengo, C. Romestant, Y. Bertin, Experimental analysis of a flat plate pulsating heat pipe with self-rewetting fluids during a parabolic flight campaign, *Acta Astronaut.* 147 (2018) 454–461.
- [15] J. Zhao, J. Qu, Z. Rao, Experiment investigation on thermal performance of a large-scale oscillating heat pipe with self-rewetting fluid used for thermal energy storage, *Int. J. Heat Mass Transf.* 108 (2017) 760–769.
- [16] Y. Naresh, K.S. Vignesh, C. Balaji, Experimental investigations of the thermal performance of self-rewetting fluids in internally finned wickless heat pipes, *Exp. Therm. Fluid Sci.* 92 (2018) 436–446.
- [17] S.M. Peyghambarzadeh, H. Hallaji, M.R. Bohloul, N. Aslanzadeh, Heat transfer and Marangoni flow in a circular heat pipe using self-rewetting fluids, *Exp. Heat Transf.* 30 (3) (2017) 218–234.
- [18] S.-C. Wu, Study of self-rewetting fluid applied to loop heat pipe, *Int. J. Therm. Sci.* 98 (2015) 374–380.
- [19] S.-C. Wu, T.-J. Lee, W.-J. Lin, Y.-M. Chen, Study of self-rewetting fluid applied to loop heat pipe with PTFE wick, *Appl. Therm. Eng.* 119 (2017) 622–628.
- [20] B. Suman, Effects of a surface-tension gradient on the performance of a micro-grooved heat pipe: an analytical study, *Microfluid. Nanofluid.* 5 (5) (2008) 655.
- [21] R.J. Moffat, Describing the uncertainties in experimental results, *Exp. Therm. Fluid Sci.* 1 (1) (1988) 3–17.
- [22] R. Boubaker, V. Platel, Vapor pocket behavior inside the porous wick of a capillary pumped loop for terrestrial application, *Appl. Therm. Eng.* 84 (2015) 420–428.
- [23] C. Ren, Q.-S. Wu, M.-B. Hu, Heat transfer with flow and evaporation in loop heat pipe's wick at low or moderate heat fluxes, *Int. J. Heat Mass Transf.* 50 (11) (2007) 2296–2308.